Variability of Marine Aerosol Fine-mode Fraction and Estimates of Anthropogenic Aerosol Component Over Cloud-free Oceans from MODIS

Hongbin Yu[1,2], Mian Chin[2], Lorraine A. Remer[2], Richard G. Kleidman[3,2], Nicolas Bellouin[4], Huisheng Bian[1,2], and Thomas Diehl[1,2]

[1] Goddard Earth Science and Technology Center, University of Maryland at Baltimore County, Baltimore, Maryland 20215
[2] Laboratory for Atmospheres, NASA Goddard Space Flight Center, Greenbelt, Maryland 20771
[3] Science System and Applications, Inc., Lanham, Maryland 20706
[4] Met Office, Hadley Centre, FitzRoy Road, Exeter, Devon, EX1 3PB, United Kingdom

Correspondence

Hongbin Yu

NASA Goddard Space Flight Center, Code 613.2
Greenbelt, Maryland 20771
Tel: (301) 614-6209   Fax: (301) 614-6307
Email: Hongbin.Yu@nasa.gov

Abstract: In this study, we examine seasonal and geographical variability of marine aerosol fine-mode fraction (f_m) and its impacts on deriving the anthropogenic component of aerosol optical depth (τ_a) and direct radiative forcing from multi-spectral satellite measurements. A proxy of f_m, empirically derived from the Moderate resolution Imaging Spectroradiometer (MODIS) Collection 5 data, shows large seasonal and geographical variations that are consistent with the Goddard Chemistry Aerosol Radiation Transport (GOCART) and Global Modeling Initiative (GMI) model simulations. The so-derived seasonally and spatially varying f_m is then implemented into a method of estimating τ_a and direct radiative forcing from the MODIS measurements. It is found that the use of a constant value for f_m as in previous studies would have overestimated τ_a by about 20% over global ocean, with the overestimation up to ~45% in some regions and seasons. The 7-year (2001-2007) global ocean average τ_a is 0.035, with yearly average ranging from 0.031 to 0.039. Future improvement in measurements is needed to better separate anthropogenic aerosol from natural ones and to narrow down the wide range of aerosol direct radiative forcing.

1.   Introduction

With the implementation of multi-wavelength, multi-angle, and polarization measuring capabilities, current satellite measurements can be used to categorize aerosol types in terms of microphysical properties, such as particle size and shape [e.g., *Kahn et al.,* 2001; *Tanré et al.,* 2001; *Higurashi and Nakajima,* 2002; *Winker et al.,* 2007]. For example, the fine-mode fraction, a measure of the contribution of fine-mode aerosols to the aerosol optical depth (AOD or τ), has been obtained from enhanced satellite sensors (e.g., the Moderate resolution Imaging Spectroradiometer - MODIS) with improved data quality [*Tanré et al.,* 1997; *Remer et al.,* 2005]. Given that anthropogenic aerosols are predominately fine-mode or in the submicron range, the fine-mode fraction in conjunction with the total aerosol optical depth can be used as a tool for separating anthropogenic aerosol from dust [*Kaufman et al.,* 2002]. *Kaufman et al.* (2005a, b) further developed a quantitative method that uses MODIS over-ocean retrievals in a consistent way to estimate the anthropogenic component (e.g., originating from industrial and urban pollution and biomass burning smoke) of aerosol optical depth, τ_a, as follows:

$$\tau_a = [(f-f_d)*\tau - (f_m-f_d)*\tau_m]/(f_a - f_d) \qquad (1)$$

where τ and f respectively represents total aerosol optical depth and fine-mode fraction retrieved directly from MODIS, both at 550 nm. Subscript *a*, *d*, and *m* denotes anthropogenic, dust, and marine aerosol components, respectively. Marine aerosol optical depth τ_m is empirically determined to be a constant of 0.06 [*Kaufman et al.,* 2005a] or a function of near-surface wind speed [*Kaufman et al.,* 2005b]. The fine-mode fractions for marine (f_m), anthropogenic (f_a), and dust (f_d) aerosol were assumed to be constant, which were then derived from Terra MODIS Collection 4 measurements in selected regions

where the specific aerosol type predominates and contributions of background aerosol are empirically accounted for [*Kaufman et al.,* 2005a]. Clearly this algorithm doesn't assume that all fine-mode AOD comes from anthropogenic contribution or anthropogenic AOD is exclusively fine-mode. Contributions from natural aerosols (dust and marine aerosol) to fine-mode AOD are empirically accounted for. The essence of this algorithm is that the MODIS data are used in a consistent way. The MODIS fine-mode fractions could be different from ground-truth values as a result of retrieval uncertainties [*Anderson et al.,* 2005a; *Kleidman et al.,* 2005]. However, by using the fine-mode fractions (f, f_m, f_a, and f_d) consistently from MODIS, one should be able to separate the components of τ_a and τ_d better than if using inconsistent values of fine-mode fraction from other sources. In parallel to *Kaufman et al.* [2005a, 2005b], *Bellouin et al.* (2005) developed a method that uses in-situ measurement-based fine-mode fraction thresholds for anthropogenic aerosol and sea salt aided by satellite-observed absorbing aerosol index to separate anthropogenic aerosol from dust and sea salt.

These satellite-based approaches have since inspired the community to further explore the use of satellites to quantify aerosol direct radiative forcing by anthropogenic aerosol [e.g., *Anderson et al.,* 2005b, *Christopher et al.,* 2006; *Yu et al.,* 2006] and to estimate trans-boundary transport of pollution aerosol [*Rudich et al.,* 2008; *Yu et al.,* 2008]. This approach, along with improvements in data sets from ground-based network and field campaigns [*Bates et al.,* 2006; *Yu et al.,* 2006; and references therein] and dedicated and coordinated efforts on aerosol modeling [*Schulz et al.,* 2006], has contributed to the reduced uncertainty of both the aerosol direct radiative forcing and

4

total anthropogenic radiative forcing as assessed in the Intergovernmental Panel on Climate Change (IPCC) Fourth Assessment Report [*Haywood and Schulz,* 2007].

Significant endeavors are needed to further investigate this approach and explore the use of satellite measurements for a better understanding of anthropogenic aerosol radiative forcing. For example, the inherent assumptions in deriving equation (1) need to be assessed and improved. In this study, we examine the assumption of constant fine-mode fraction for marine aerosol (f_m) and propose a self-consistent approach to improve the characterization of seasonal and spatial variations of f_m. Over remote oceans, aerosols are generated from bursting bubbles that inject sea salt particles, dimethylsulfide (DMS) and organic matters into the marine boundary layer. The DMS oxidation produces SO_2 and sulfates. The organic particles and DMS-oxidized sulfates contribute to the optical depth predominantly in the sub-micron range. The sea salt aerosols have much broader size distributions, with mass concentrated in the super-micron size range. The sub-micron sea salt is, however, much more efficient in scattering the solar radiation. As a result, the sub-micron sea salt constitutes a significant contributor to the sea salt optical depth and also an important component of fine-mode marine aerosol optical depth [*Bates et al.,* 2001]. The amount, composition, and size of marine-generated aerosols should depend on a variety of atmospheric and oceanic parameters, such as biological activities of ocean, sea-surface temperature, ocean upwelling, near-surface wind speed, atmospheric oxidizing capacity, among others [*O'Dowd et al.,* 2004; *Leck and Bigg,* 2005]. This complexity would result in large seasonal and geographical variations of f_m,

as can be inferred from some observations [e.g., *Wilson and Forgan,* 2002; *Shinozuka et al.,* 2004].

In section 2, we derive f_m from the Terra MODIS Collection 5 (C5) data and discuss its seasonal and geographical variations in conjunction with the Goddard Chemistry Aerosol Radiation Transport (GOCART) and Global Modeling Initiative (GMI) model simulations of marine aerosol. The derived marine fine-mode fraction, which is seasonally and geographically varying, is then utilized to derive the anthropogenic aerosol optical depth from 2001-2007 MODIS observations. Section 3 examines the seasonal and interannual variability of τ_a and its comparisons with model simulation and previous studies. Major results and conclusions are summarized in section 4.

2.   Marine aerosol fine-mode fraction from MODIS: Seasonal and geographical variations

MODIS C5 aerosol retrievals with consistent algorithms have recently become available [*Remer et al.,* 2006, 2008; *Levy et al.,* 2007]. Because values of the aerosol fine-mode fraction are sensitive to details of the algorithm and MODIS calibration, it warrants a re-assessment of the fine-mode fractions for anthropogenic, dust, and marine aerosol in order to apply the method of *Kaufman et al.* (2005a,b) to MODIS C5. *Jones and Christopher* (2007), hereafter referred to as JC07, derived the fine-mode fraction values for anthropogenic, dust, and sea salt aerosol from 1-year Terra MODIS C5 data, with aerosol type characterization guided by GOCART model simulations. Here we

follow the method as described in *Kaufman et al.* (2005a,b) by selecting the representative regions and seasons dominated by pollution (i.e., North Atlantic off the coast of New England in summer), dust (i.e., North Atlantic off the coast of North Africa in summer), and marine aerosol (i.e., south to Australia) to the Terra MODIS C5 Level 3 daily data (at a resolution of 1°x1°) from 2001-2007. When deriving fine-mode fractions for dust and pollution, a contribution by marine aerosol is empirically excluded [*Kaufman et al.,* 2005a]. **Table 1** lists the newly derived representative values of fine-mode fraction for individual aerosol types and their comparisons with those derived from Terra MODIS Collection 4 (C4) data [*Kaufman et al.,* 2005a,b]. The fine-mode fraction for mineral dust as derived from C5 is smaller than that from C4, while that for marine aerosol shows the opposite relationship. For pollution aerosol, the fine-mode fraction is similar between C5 and C4. These differences result from assumptions about the optical properties of coarse-mode particles that were adjusted to better match more recent observations in C5 algorithm [*Remer et al.,* 2008]. The consequence of this algorithm change is to reduce the positive bias in the fine-mode fraction retrieved by C4 [*Kleidman et al.,* 2005; *Remer et al.,* 2008].

Our derived fine-mode fractions values are different from those derived by JC07. JC07 derived fine-mode fraction is 0.83, 0.44, and 0.25 for anthropogenic, dust, and sea salt aerosol, respectively. Differences between this study and JC07 could have resulted from several possible factors. First, JC07 derived these values over much broader areas than this study does and the differences between the two studies may have come from spatial variability of particle size for a specific aerosol type. It is also possible that

MODIS and GOCART differ in the characterization of aerosol types. Second, while JC07 used monthly MODIS C5 data, we are using MODIS C5 daily 1°x1° data in this study. Third, it is expected that the fine-mode fraction for sea salt in JC07 is smaller than the derived value for marine aerosol in this study because of the exclusion of contribution of submicron sulfate produced from DMS in JC07. Note also that the sea salt fine-mode fraction in JC07 may be biased low because of cloud contamination [*Zhang et al.,* 2005] and unaccounted-for whitecaps over the "roaring forties". Fourth, contribution of background marine aerosol was accounted for in this study but not accounted for in JC07 when deriving the fine-mode fractions for anthropogenic aerosol and dust. This difference may partly explain larger fine-mode fraction for anthropogenic aerosol derived in this study.

By applying equation (1) with these new values of f_m, f_d, and f_a (in Table 1) to the MODIS C5 data, we obtain the global ocean average anthropogenic AOD of 0.040, which is about 20% larger than the average (0.033) or is at the upper bound (with an estimated uncertainty of 30%) as derived from MODIS C4 [*Kaufman et al.,* 2005a]. This is opposite to the study by *Bellouin et al.* (2008) that show a 25% decrease of anthropogenic AOD over ocean when updating from C4 to C5. Since the same thresholds of the fine-mode fraction were used to separate aerosol types for both C5 and C4 in *Bellouin et al.* [2005, 2008], the reduced fine-mode fraction over oceans in C5 [*Remer et al.,* 2008] results in the smaller anthropogenic AOD derived from C5 [*Bellouin et al.,* 2008] than that from C4 [*Bellouin et al.,* 2005].

As discussed earlier, marine aerosol fine-mode fraction should present large spatial and seasonal variations and a use of constant f_m could introduce large errors to the derived anthropogenic aerosol optical depth and direct radiative forcing. Here we derive the climatology of seasonal average fine-mode fraction for background marine aerosol by averaging 2001-2007 Terra/MODIS daily fine-mode fraction weighted by τ for $0.03 < \tau < 0.10$ in individual $1° \times 1°$ grids. We assume that f_m has relatively small inter-annual variability and the multi-year data are then used to obtain a better spatial coverage. It is also required that the number of available daily measurements in each $1° \times 1°$ grid box during a season is no less than 10 for calculating a seasonal average. The lower bound of τ is set to exclude data with relatively large uncertainties, while the upper bound of τ is chosen for a compromise of excluding continental influences but acquiring adequate spatial coverage. Note that $\tau < 0.03$ accounts for ~10% of all over-ocean data [*Remer et al.*, 2008]. Spatial gaps in the derived f_m shrink or expand respectively with increasing or decreasing the upper bound of τ near coasts of major continental aerosol source regions. For the selected τ range, continental influences are likely to exist. However such residual continental influence appears to have a small effect on the derived f_m. As shown in **Figure 1**, for example, by varying the upper bound of τ from 0.1 to 0.15, the difference of the derived f_m in individual grids is predominantly (~98.5%) within ±0.1, in which ~80% is within ±0.05.

Kaufman et al. [2001] derived the climatology of optical depth and properties of the baseline marine aerosol from multi-year measurements of nine Aerosol Robotic Network (AERONET) stations. The f_m at 500 nm is about 0.64 over the Atlantic

(averaged over five stations) and 0.56 over the Pacific (averaged over four stations) (Table 2 in *Kaufman et al.,* 2001). By extracting values from the derived f_m climatology in this study for those stations, we get f_m at 550 nm of 0.58±0.11 over the Atlantic and 0.54±0.05 over the Pacific, which is in good agreement with that of *Kaufman et al.* [2001]. Given the difficulty in obtaining spatial and temporal variations of the fine-mode fraction of marine aerosol from other measurements, we examine simulations of two global chemical transport models in this study, namely GOCART and GMI. To model marine aerosol, we only consider emissions of sea salt and DMS from ocean and volcanic SO_2. The sulfate produced from DMS and volcanic emissions and sub-micron sea salt are categorized into "fine mode" in calculating the fine-mode fraction for the marine aerosol. GOCART takes into account both eruptive and non-eruptive volcanic sources [*Chin et al.,* 2000a, 2002], whereas GMI only includes non-eruptive volcanoes. Processes represented in the models are chemistry, convection, advection, boundary layer mixing, dry and wet deposition, gravitational settling, and hygroscopic growth of aerosol particles. Despite being driven by same meteorological and photochemical fields, the two models differ in the oceanic DMS and volcanic SO_2 emissions, and parameterizations of several processes that determine aerosol such as aqueous phase reactions, dry and wet deposition, gravitational settling, and convective transport [*Chin et al.,* 2000a,b, 2002; *Bian et al.,* 2008]. Thus the simulated marine fine-mode fraction can still be different between the two models.

Figure 2 shows the MODIS-derived f_m and its comparisons with GOCART and GMI simulations. Differences of 0.1-0.2 exist between the MODIS-based f_m and model

simulations in some regions, which however would generally fall within the uncertainty ranges of either method. All three sets of f_m show generally consistent, pronounced seasonal and geographical variations. The marine fine-mode fraction is larger in summer than in winter, and also larger in tropical and coastal regions than in high latitudes and remote oceans. These seasonal and spatial variations result from a complicated interplay of several ocean and atmosphere processes that determine the loading of sea salt and marine sulfate. Sea salt particles are generated via the bubble-bursting process, with a higher production rate primarily associated with strong wind speed [e.g., *Shinozuka et al.,* 2004]. Factors that determine the sulfate loading are associated with ocean DMS production, emission of DMS to the marine boundary layer, and chemical transformation of DMS to SO_2 and sulfate. The in-water DMS production is highly correlated with the intensity of phytoplankton activities that depends on ocean upwelling, availability of iron, among others [e.g., *Liss,* 2007]. Since DMS is saturated in most surface ocean waters, the DMS flux to the atmosphere is determined by the air-sea transfer rate depending on seawater DMS concentrations, near-surface wind speed, and atmospheric stability. In the atmosphere, DMS is transformed to SO_2 and sulfate through oxidation by the OH radical (day) and NO_3 (night), with a rate depending on the atmospheric oxidizing capacity that is stronger in summer and in the tropics.

3.   Updated estimates of anthropogenic aerosol optical depth

The large spatial and temporal variations of f_m suggest that a use of constant f_m could introduce large uncertainties in the derived τ_a and direct radiative forcing, depending on season and region. Here we use the MODIS-based climatology of seasonal

average f_m shown in Figure 2 and f_a and f_d from Table 1 to derive the anthropogenic

aerosol optical depth from Terra/MODIS Collection 5. Spatial gaps in MODIS f_m as

shown in Figure 2 (excluding gaps in high latitudes where MODIS aerosol retrievals are

not available and hence anthropogenic aerosol optical depth can't be derived) are filled

with GOCART simulations by simply scaling the GOCART simulation of f_m with the

average MODIS/GOCART ratio in selected regions surrounding the data gaps. Using

GOCART to fill in gaps for MODIS does introduce additional uncertainty to the final

estimates. However it is still a 'reasonable' step to take in order to obtain a global picture

because on an annual average, the model-assisted piece accounts for only about 5% of the

oceans. Other assumptions are the same as that in *Kaufman et al.* (2005a).

Figure 3a shows distributions of seasonal average τ_a over 2001-2007 data period.

Evident from these plots are several pronounced continental outflows from major

industrial pollution and biomass burning regions. For example, pollution and biomass

burning aerosols from Asia and Europe sweep across the North Pacific basin during the

boreal spring and summer. Tropical biomass burning smoke is transported to surrounding

oceans during the austral winter (JJA) and spring (SON). North American pollution is

transported to Europe in summer. Pollution from the Indian subcontinent spreads to the

northern Indian Ocean in pre-monsoon season. Central America fires contribute aerosols

to the eastern tropical Pacific. High values of τ_a over Southern Oceans are most likely

artifacts because of large uncertainties of MODIS retrievals in the region [*Zhang et al.*,

2005; *Smirnov et al.,* 2006]. The 7-year global (excluding some high latitudes where data

are not available) ocean average τ_a is 0.035, with annual average ranging from 0.031 to

0.039. Seasonal averages of anthropogenic AOD, along with those for fine-mode fraction and anthropogenic fraction (a ratio of τ_a to τ), were calculated over ocean in 13 zones (following *Yu et al.,* 2006), as shown in **Figure 3b**.

Figure 4 compares the derived anthropogenic AOD using spatially and seasonally varying f_m (Figure 2a and 2b) against that using a constant f_m (0.45) from Table 1 for the same MODIS Terra C5 data. Each of 52 data points represents a seasonal average in each of the 13 zones defined in Figure 3b. Only in a few regions during some seasons does the use of constant f_m yields τ_a lower than the use of variable f_m, including high latitudes of North Pacific and North Atlantic during winter, Arabian Sea during summer, and Southern Oceans during summer and fall. In all other regions and seasons, the constant f_m assumption results in higher τ_a up to about 45%. On average, the τ_a derived from constant f_m is nearly 20% higher than that derived from variable f_m.

The derived anthropogenic aerosol optical depth is subject to uncertainties associated with parameters in Eq. (1). While rigorous validation of the MODIS-derived τ_a is difficult because of dearth of in-situ measurements, here we provide an empirical estimate of the uncertainty associated with τ_a. We first empirically determine uncertainties for major parameters based on previous studies of satellite validations and in-situ measurements [e.g., *Bellouin et al.,* 2005; *Remer et al.,* 2005, 2006; *Smirnov et al.,* 2002], as listed in **Table 2**. Note that fine-mode fractions for individual aerosol types are derived from the MODIS observations in this study. As such the error associated with MODIS fine-mode fraction, if not strongly dependent on aerosol type, could be largely

13

offset by those associated with fine-mode fractions for individual aerosol types and hence is not included in our uncertainty analysis separately. We then apply the perturbation to each parameter accordingly while using default values for other parameters and re-derive the anthropogenic AOD for the whole year of 2002. The corresponding uncertainties for τ_a are then calculated and listed in Table 2 by comparing the perturbations with the default. For a fractional uncertainty of x, the corresponding uncertainty factor (UF) is 1+x. By assuming the probability distribution function for each factor is log normal and individual uncertainties are independent [*Penner et al.,* 1994], we estimate the overall uncertainty factor of 1.52 for τ_a derived in this study. This suggests that the global ocean average τ_a ranges from 0.023 - 0.053.

Aerosols can have pronounced seasonal variations on a regional scale, as determined by emissions, chemical transformation, atmospheric transport, and removal processes. **Figure 5** shows the derived 7-year (2001-2007) average seasonal cycle of anthropogenic aerosol optical depths over northern mid-latitude (30°N-60°N), northern tropical (Equator-30°N), southern tropical (30°S-Equator), and global (60°S-60°N) oceans. In 30°N-60°N where anthropogenic aerosol is dominated by outflow of industrial and urban pollution (with some contributions from boreal forest fires in summer), the anthropogenic AOD is about 2 times larger in spring and summer than in winter and fall. Over tropical oceans (Equator-30°N and 30°S-Equator) where anthropogenic aerosol is dominated by biomass burning smoke, the AOD peak occurs in spring (e.g., March-April-May for the northern tropical oceans and September-October-November for the

southern tropical oceans). Different seasonal variations of AOD in different latitude bands offset each other, resulting in no clear seasonal variation on a global ocean basis.

Figure 6 shows interannual variations of seasonal average anthropogenic aerosol optical depth over the 7-year period in individual regions corresponding to the divisions used in Figure 5. Given that large seasonal variations could mask any potential tendency of changes over the period, the anthropogenic AOD in Figure 6 has been de-seasonalized using the 7-year average seasonal cycle as shown in Figure 5. A linear regression is performed for the variation of average anthropogenic AOD with time, shown as solid line in the figure along with calculated regression equation and correlation coefficient (R^2). In the northern mid-latitudes (Figure 6a), there was a much elevated value of anthropogenic AOD in spring 2003, and a relatively small elevation in summer 2003, corresponding to record intense Siberian forest fires [*Goldammer et al.,* 2004; *Wotawa et al.,* 2006]. Statistical analysis suggests no clear tendency of AOD change over the period (correlation as low as 0.05). A further examination of two sub-regions in the northern mid-latitudes, namely the northwestern Pacific (30°N-60°N, 115°E-180°E) and North Atlantic (30°N-60°N, 70°W-20°E), does not yield higher correlations or clearer tendencies of change. On the contrary, the anthropogenic AOD shows a statistically significant (i.e., R^2 of ~0.4), increasing tendency over the 7-year period in the tropical oceans (Figure 6b and 6c). In Equator-30°N latitudes, τ_a increases at a rate of 0.0005 τ/season (or 0.002 τ/a). In 30°S-Equator latitudes, the increasing rate of τ_a is 0.0003 τ/season (or 0.0012 τ/a), which is roughly half of its northern counterpart. On a global ocean average (Figure 6d), τ_a shows an increasing tendency at a rate of 0.0012 τ/a, but

15

with a smaller correlation of $R^2 = 0.27$. The above analysis may suggest that biomass

burning emissions and fossil fuel consumptions in tropical regions may have been

increasing during 2001-2007. On the other hand, some other factors such as the sensor

calibration and retrieval uncertainty may also contribute to the change; and future efforts

are needed to quantify them. The data record from MODIS is also too short to derive

long-term trends of aerosols.

How well does the derived anthropogenic aerosol optical depth compare with

other measurement-based estimates and model simulations? *Bellouin et al.* (2005) use

prescribed, in-situ measurement-based thresholds of fine-mode fraction f (f>0.83 for

pollution-dominated aerosol, f<0.35 for dust and sea salt mixture, and in between for

pollution, dust, and sea salt mixture) aided by the Total Ozone Mapping

Spectroradiometer (TOMS) absorbing aerosol index (AAI) to separate anthropogenic

aerosol from mineral dust and sea salt. Background sea salt AOD is subtracted by using

an empirical AOD-dependence on surface wind speed. The method was originally

applied to MODIS C4 [*Bellouin et al.,* 2005] and most recently to MODIS C5

measurements for updated estimates of the anthropogenic aerosol optical depth and direct

radiative forcing [*Bellouin et al.,* 2008] (hereafter referred to as B08). Although B08

uses the same MODIS C5 measurements as this study does, the two studies use different

criteria and approach to separate anthropogenic aerosol from dust and marine aerosol.

Figure 7 compares the annual average anthropogenic aerosol optical depth over oceans

derived in this study (Figure 7a) with that from B08 (Figure 7b). While the two

approaches give similar spatial patterns, some major differences do exist on regional

scales. On one hand, off the coast of North Africa the anthropogenic outflow derived in this study is smaller in magnitude and less extensive in space than that from B08. The annual average τ_a over 0°-20°N and 40°W-10°E is 0.034 from this study, which is a factor of 2-3 smaller than 0.087 from B08. On the other hand, B08 derives weaker pollution outflows over North Pacific and North Atlantic than this study does. The relatively large τ_a over Southern Ocean as shown in Figure 7(a) would be an artifact resulting from the relatively poor quality of MODIS retrievals and our simplified representation of marine AOD in such regimes with strong winds and high fractions of cloud [*Zhang et al.,* 2005; *Smirnov et al.,* 2006]. On annual and global (again averaged only over where measurements are available) basis, the average τ_a is estimated to be 0.032 in this study, which is substantially larger than 0.021 of B08. When the estimated uncertainty factor of 1.52 discussed earlier is applied to our estimate, the B08 estimate is consistent with the low bound of anthropogenic AOD of this study.

A number of factors should contribute to such differences. For example, it is likely that B08 may have missed some pollution outflow far from coastal regions (e.g., North Atlantic and North Pacific) when the pollution contribution is not large enough to elevate the MODIS fine-mode fraction to the prescribed high threshold (i.e., 0.83) for anthropogenic aerosol. The use of TOMS absorbing aerosol index would not help in these cases for separating pollution from dust and sea salt, because of weak sensitivity of TOMS to these pollution plumes at relatively low altitude and with weak ultraviolet (UV) absorption. The examined large difference off the coast of North Africa influenced by both dust and smoke may manifest the difficulty in separating smoke from dust from

space. Given that B08 uses a lower f value as a threshold of for categorizing "pure"

smoke or pollution than we are using, their smoke AOD would be larger than that from

this study. For a smoke-dust mixture (i.e., $0.35 < f < 0.83$), smoke is separated from dust by

using f as an approximation for the fraction of smoke in B08. Inherent in this

approximation is that fine-mode aerosol comes exclusively from smoke, which could

overestimate the smoke AOD because a fine-mode fraction of dust is not negligible.

These differences in algorithms of separating smoke from dust are thus likely to result in

smaller and less extensive smoke outflow from North Africa in this study than in B08. As

an exercise we re-derive the anthropogenic AOD by using the thresholds recommended

in B08 for f_a (=0.83) and f_d (= 0.35) and also reducing the f_m by half. This yields an

average anthropogenic AOD of 0.073 over 0°-20°N and 40°W-10°E, much closer to

0.087 from B08. However, the global average anthropogenic AOD using these modified

parameters would increase by about 70% to 0.058, resulting in much larger discrepancies

against 0.021 of B08. This exercise suggests the complexity of separating anthropogenic

aerosol from natural one. There is a need to examine potential temporal and spatial

variations of fine-mode fraction for pollution and dust. In-situ measurements, presumably

more accurate than the satellite-based estimates (e.g., Table 1), should be collected to

facilitate understanding of uncertainties associated with satellite measurements and hence

developing a strategy of integrating in-situ and satellite measurements without

introducing additional uncertainties resulting from possible discrepancies between the

two measurements.

Our estimated ocean average anthropogenic AOD is also about 50% larger than 0.021 from an ensemble of seven model simulations from the Aerosol Comparison between Observations and Models (AeroCom) group [*Schulz et al.,* 2006]. Such differences can be at least partially attributed to different definitions used in the two studies. While anthropogenic aerosol is defined as a difference between present-day and pre-industrial simulations in *Schulz et al. [2006]*, it is defined in the satellite-based studies as a difference between present-day total aerosol and natural aerosol with an assumption that biomass burning aerosol is completely man made. Given that part of biomass burning aerosol is of natural origin and should have occurred in pre-industrial era, the value from *Schulz et al.* [2006] should be reasonably smaller than the satellite-based estimates. An adequate assessment of such difference in the definition of anthropogenic aerosol is needed to get a quantitative understanding of the apparent discrepancies in current estimates of anthropogenic aerosol optical depth [*Bellouin et al., 2*008].

Here we compare the MODIS-based anthropogenic AOD with GOCART simulations using the similar definition of anthropogenic aerosol, i.e., a difference between present-day total aerosol and present-day natural aerosol. The GOCART model was run twice, once with all aerosol sources and then without anthropogenic and biomass burning sources. A difference between the two runs is used to represent anthropogenic aerosol, as shown in Figure 7c. Here we have assumed that biomass burning aerosols are completely man-made, which is also somewhat consistent with the assumption made for the satellite-based estimates. In general, GOCART simulations show higher τ_a than both

satellite-based approaches in most regions. On a global average, the average of 0.030 from GOCART simulations is consistent with the estimate from this study to about 10%, but is about 50% higher than B08 and *Schulz et al.* [2006]. On regional scales, the model-satellite difference depends on the method of satellite-based estimates. On one hand, off the coast of North Africa (0°-20°N, 40°W-10°E) the GOCART simulations give an average of 0.093 for the anthropogenic AOD, which is close to B08 but is nearly a factor of 3 larger than this study. On the other hand, the model simulations of pollution outflow over North Pacific and North Atlantic are consistent with this study, but much stronger than B08.

4.   Concluding remarks

Marine aerosol fine-mode fraction is determined by a number of factors associated with the state of atmosphere and ocean. In this study, we have derived empirically the fine-mode fraction for background marine aerosol, f_m, from the MODIS Collection 5 over-ocean measurements. This MODIS-based f_m shows large seasonal and geographical variations that are generally consistent with GOCART and GMI simulations of marine aerosol. The seasonally and spatially varying f_m has been implemented into the method of deriving anthropogenic AOD from MODIS observations [*Kaufman et al.,* 2005a]. It is found that a use of constant f_m as did in previous studies [*Kaufman et al.,* 2005a, b] would have overestimated the anthropogenic AOD over global ocean by nearly 20%, with the overestimate up to ~45% for some regions and seasons. It is estimated that the 7-year (2001-2007) global (where MODIS measurements are available) ocean average anthropogenic AOD (τ_a) is 0.035, which is consistent with GOCART simulation

but about 50% larger than the satellite-based estimate by *Bellouin et al.* (2008). The derived 7-year anthropogenic AOD over tropical oceans (dominated by biomass burning smoke) shows a tendency of increase at a rate of 0.002 (northern tropical ocean) and 0.001 (southern tropical ocean) τ_a/a from 2001 to 2007. In Northern Hemisphere mid-latitudes dominated by industrial and urban pollution, there is no statistically significant tendency of increase or decrease.

As discussed earlier in this study, current methods of deriving anthropogenic aerosol component have used exclusively the MODIS aerosol data with differences in specifics of the approaches and the derived global ocean anthropogenic AOD can still differ by about 50%. Estimating the anthropogenic aerosol component over land is even more difficult because of larger uncertainties in aerosol retrievals than over ocean. The aerosol forcing efficiency, defined as aerosol direct forcing per unit of τ_a and a useful quantity for calculating the aerosol direct forcing, is mainly governed by aerosol size distribution and chemical composition (determining the aerosol single-scattering albedo and phase function), surface reflectivity, and solar geometry [*Zhou et al.,* 2005]. Current estimates of global ocean average anthropogenic aerosol forcing efficiency also differ substantially, ranging from nearly -30 $\text{Wm}^{-2}\,\tau_a^{-1}$ to greater than -40 $\text{Wm}^{-2}\,\tau_a^{-1}$ [*Bellouin et al.,* 2005; *Christopher et al.,* 2006; *Kaufman et al.,* 2005a; *Quaas et al.,* 2008; *Remer and Kaufman,* 2006; *Schulz et al.,* 2006; *Yu et al.,* 2004, 2006; *Zhao et al.,* 2008]. On regional scales, uncertainty ranges for τ_a and forcing efficiency can be much larger than the global averages. To narrow down the uncertainty range, substantial effort is required in the future. It will be helpful to evaluate the MODIS-based estimates by developing

independent approaches using data sets from other satellite sensors, e.g., measurements of particle shape and size from the Multiangle Imaging SpectroRadiometer (MISR) [*Kahn et al.,* 2001] and the Cloud-Aerosol Lidar and Infrared Pathfinder Satellite Observations (CALIPSO) [*Winker et al.,* 2007]. Future satellite measurements should focus on improved retrievals of such aerosol properties as size distribution, particle shape, and absorption, along with algorithm refinement for better AOD retrievals. It is also strategically needed to conduct *in situ* measurements that allow for the characterization of anthropogenic AOD or anthropogenic fraction in context of evaluating or validating satellite remote sensing measurements of the atmospheric column. Finally, the better determination of anthropogenic aerosols also requires a quantification of biomass burning ignited by lightning (natural origin) and mineral dust due to human induced changes of land cover/land use and climate (anthropogenic origin).

References:

Anderson, T.L., Y. Wu, D.A. Chu, B. Schmid, J. Redemann, and O. Dubovik (2005a):

Testing the MODIS satellite retrieval of aerosol fine-mode fraction, *J. Geophys. Res.,
110,* D18204, doi:10.1029/2005JD005978.

Anderson, T.L., et al., (2005b), A-Train strategy for quantifying direct climate forcing by

anthropogenic aerosols, *Bull. Amer. Meteorolo. Soc., 86(12),* 1795-1809.

Bates, T.S., et al. (2006), Aerosol direct radiative effects over the northwest Atlantic,

northwest Pacific, and North Indian Oceans: estimates based on in-situ chemical and

optical measurements and chemical transport modeling, *Atmos. Chem. Phys., 6,*
1657-1732.

Bates, T.S., et al. (2001), Regional physical and chemical properties of the marine

boundary layer aerosol across the Atlantic during Aerosols99: An overview, *J.
Geophys. Res., 106(D18),* 20767-20782.

Bellouin, N, O. Boucher, J. Haywood, and M.S. Reddy (2005), Global estimate of aerosol

direct radiative forcing from satellite measurements, *Nature, 438 (7071),* 1138-1141,
doi:10.1038/nature04348.

Bellouin, N., A. Jones, J. Haywood, and S.A. Christopher (2008), Updated estimate of

aerosol direct radiative forcing from satellite observations and comparison against

the Hadley Centre climate model, *J. Geophys. Res., 113,* D10205,
doi:10.1029/2007JD009385.

Bian, H., M. Chin, J. Rodriguez, H. Yu, J.E. Penner, S. Strahan (2008), Sensitivity of

aerosol optical thickness and aerosol direct radiative effect to relative humidity,

Atmos. Chem. Phys. Discuss., 8, 13233-13263.

Chin, M., R. B. Rood, S.-J. Lin, J. F. Muller, and A. M. Thomspon (2000a), Atmospheric sulfur cycle in the global model GOCART: Model description and global properties, *J. Geophys. Res., 105,* 24,671-24,687.

Chin, M., D. Savoie, B. J. Huebert, et al. (2000b), Atmospheric sulfur cycle in the global model GOCART: Comparison with field observations and regional budgets, *J. Geophys. Res., 105,* 24,689-24,712.

Chin, M., P. Ginoux, S. Kinne, et al. (2002), Tropospheric aerosol optical thickness from the GOCART model and comparisons with satellite and sunphotometer measurements, *J. Atmos. Sci., 59,* 461-483.

Christopher, S.A., J. Zhang, Y.J. Kaufman, and L.A. Remer (2006), Satellite-based assessment of top of atmosphere anthropogenic aerosol radiative forcing over cloud-free oceans, *Geophys. Res. Lett.*, *33,* L15816, doi:10.1029/2005GL025535.

Goldammer, J.G., A. Sukhinin, and I, Csiszar (2004), The current fire situation in the Russian Federation: Implications for enhancing international and regional cooperation in the UN framework and the global programs on fire monitoring and assessment, *Int. Forest Fire News, 29,* 89-111.

Haywood, J., and M. Schulz (2007), Causes of the reduction in uncertainty in the anthropogenic radiative forcing of climate between IPCC (2001) and IPCC (2007), *Geophys. Res. Lett., 34,* L20701, doi:10.1029/2007GL030749.

Higurashi, A., and T. Nakajima (2002), Detection of aerosol types over the East China Sea near Japan from four-channel satellite data, *Geophys. Res. Lett., 29(17), 1836,* doi:10.1029/2002GL015357.

Kahn, R., P. Banerjee, and D. McDonald (2001), The sensitivity of multiangle imaging to natural mixtures of aerosols over ocean. *J. Geophys. Res., 106,* 18219-18238.

Kaufman, Y.J., O. Boucher, D. Tanré, M. Chin, L.A. Remer, and T. Takemura (2005a), Aerosol anthropogenic component estimated from satellite data. *Geophys. Res. Lett. 32, L17804,* doi:10/1029/2005GL023125.

Kaufman, Y.J., I. Koren, L.A. Remer, D. Tanré, P. Ginoux, and S. Fan (2005b), Dust transport and deposition observed from the Terra-Moderate Resolution Imaging Spectroradiometer (MODIS) spacecraft over the Atlantic Ocean, *J. Geophys. Res., 110, D10S12,* doi:10.1029/2003JD004436.

Kaufman, Y. J., J. M. Haywood, P. V. Hobbs, W. Hart, R. Kleidman, and B. Schmid (2003a), Remote sensing of vertical distributions of smoke aerosol off the coast of Africa. *Geophys. Res. Lett.*, *30(D16), 1831,* doi: 10.1029/2003GL017068.

Kaufman, Y. J., D. Tanré, and O. Boucher (2002), A satellite view of aerosols in the climate system. Review. *Nature*, *419,* 215-223.

Kleidman, R.G., et al. (2005), Comparison of Moderate Resolution Imaging Spectroradiometer (MODIS) and Aerosol Robotic Network (AERONET) remote-sensing retrievals of aerosol fine mode fraction over ocean, *J. Geophys. Res.*, *110,* D22205, doi:10.1029/2005JD005760.

Leck, C., and E.K. Bigg (2005), Source and evolution of the marine aerosol – A new perspective, *Geophys. Res. Let., 32, L19803,* doi:10.1029/2005GL023651.

Levy, R., L.A. Remer, S. Mattoo, E. Vermote, and Y. Kaufman (2007), Second-generation algorithm for retrieving aerosol properties over land from MODIS spectral reflectance, *J. Geophys. Res., 112*, D13211, doi:10.1029/2006JD007811.

Liss, P.S., Trace gas emissions from the marine biosphere, *Phil. Trans. R. Soc. A., 365,* 1697-1704, 2007.

O'Dowd, C., et al. (2004), Biogenically-driven organic contribution to marine aerosol, *Nature, 431,* 676-680.

Penner, J., R. Charlson, J. Hales, et al. (1994): Quantifying and minimizing uncertainty of climate forcing by anthropogenic aerosols, *Bull. Amer. Meteorolo. Soc.,* 75, 375-400.

Quaas, J., O. Boucher, N. Bellouin, and S. Kinne (2008), Satellite-based estimate of the direct and indirect aerosol climate forcing, *J. Geophys. Res., 113,* D05204, doi:10.1029/2007JD008962.

Remer, L.A., Y.J. Kaufman, D. Tanré, et al. (2005), The MODIS aerosol algorithm, products, and validation, *J. Atmos. Sci., 62,* 947-973.

Remer, L.A., D. Tanré, Y.J. Kaufman, R.C. Levy, and S. Mattoo (2006), Algorithm for remote sensing of tropospheric aerosol from MODIS: Collection 005, Algorithm Theoretical Basis Document available at http/://modis-atmos.gsfc.nasa.gov/reference_atbd.php.

Remer, L.A., and Y.J. Kaufman (2006), Aerosol direct radiative effect at the top of the atmosphere over cloud free ocean derived from four years of MODIS data. *Atmos. Chem. Phys., 6,* 237-253.

Remer, L.A., R.G. Kleidman, R.C. Levy et al. (2008), An emerging aerosol climatology from the MODIS satellite sensors, *J. Geophys. Res., 113,* D14S07, doi:10.1029/2007JD009661.

Rudich, Y., Y.J. Kaufman, U. Dayan, H. Yu, and R.G. Kleidman (2008), Estimation of transboundary transport of pollution aerosols by remote sensing in the eastern Mediterranean, *J. Geophys. Res., 113,* D14S13, doi:10.1029/2007JD009601.

Schulz, M., C. Textor, S. Kinne, et al. (2006), Radiative forcing by aerosols as derived from the AeroCom present-day and pre-industrial simulations, *Atmos. Chem. Phys.*, *6*, 5225-5246.

Shinozuka, Y., A.D. Clarke, S.G. Howell, V.N. Kapustin, and B.J. Huebert (2004), Sea-salt vertical profiles over the Southern and tropical Pacific oceans: Microphysics, optical properties, spatial variability, and variations with wind speed, *J. Geophys. Res., 109,* D24201, doi:10.1029/2004JD004975.

Smirnov, A., B.N. Holben, Y.J. Kaufman, O. Dubovik, T.F. Eck, I. Slutsker, C. Pietras, and R.N. Halthore (2002), Optical properties of atmospheric aerosol in maritime environments, *J. Atmos. Sci., 59,* 501-523.

Smirnov, A., B. N. Holben, S. M. Sakerin, D. M. Kabanov, I. Slutsker, M. Chin, T. L. Diehl, L. A. Remer, R. Kahn, A. Ignatov, L. Liu, M. Mishchenko, T. F. Eck, T. L. Kucsera, D. Giles, and O. V. Kopelevich (2006), Ship-based aerosol optical depth measurements in the Atlantic Ocean: Comparison with satellite retrievals and GOCART model. *Geophys. Res. Lett., 33,* L14817, doi: 10.1029/2006GL026051.

Tanré, D., Y. J. Kaufman, M. Herman, and S. Mattoo (1997), Remote sensing of aerosol properties over oceans using the MODIS/EOS spectral radiances. *J. Geophys. Res.*, *102,* 16971-16988.

Tanré, D., F.M. Bréon, J.L. Deuzé, M. Herman, P. Goloub, F. Nadal, and A. Marchand (2001), Global observation of anthropogenic aerosols from satellite, *Geophys. Res. Lett., 28(24),* 4555-4558.

Wilson, S.R., and B.W. Forgan (2002), Aerosol optical depth at Cape Grim, Tasmania, 1986-1999. *J. Geophys. Res., 107*, 4068, doi:10.1029/2001JD000398.

W Winker, D., W.H. Hunt, and M.J. McGill (2007), Initial performance assessment of CALIOP, *Geophys. Res. Lett., 34,* L19803, doi:10.1029/2007GL030135.

Wotawa, G., L.-E. De Geer, A. Bekcer, R. D'Amours, M. Jean, R. Servranckx, and K. Ungar (2006), Inter- and intra-continental transport of radioactive cesium released by boreal forest fires, *Geophys. Res. Lett., 33,* L12806, doi:10.1029/2006GL026206.

Yu, H., R.E. Dickinson, M. Chin, Y.J. Kaufman, M. Zhou, L. Zhou, Y. Tian, O. Dubovik, and B.N. Holben (2004), The direct radiative effect of aerosols as determined from a combination of MODIS retrievals and GOCART simulations, *J. Geophys. Res., 109,* D03206, doi:10.1029/2003JD003914.

Yu, H., Y.J. Kaufman, M. Chin, et al. (2006), A review of measurement-based assessments of the aerosol direct radiative effect and forcing, *Atmos. Chem. Phys., 6,* 613-666.

Yu, H., L.A. Remer, M. Chin, H. Bian, R.G. Kleidman, and T. Diehl (2008), A satellite-based assessment of trans-pacific transport of pollution aerosol, *J. Geophys. Res., 113,* D14S12*,* doi:10.1029/2007JD009349.

Zhang, J., J. S. Reid, and B. N. Holben (2005), An analysis of potential cloud artifacts in MODIS over ocean aerosol optical thickness products, *Geophys. Res. Lett., 32,* L15803, doi:10.1029/2005GL023254.

Zhao, T. X.-P., H. Yu, I. Laszlo, M. Chin, and W.C. Conant (2008), Derivation of component aerosol direct radiative forcing at the top of atmosphere for clear-sky oceans, *J. Quant. Spectro. Rad. Trans.*, *109(7),* 1162-1186.

Zhou, M., H. Yu, R.E. Dickinson, O. Dubovik, and B.N. Holben (2005), A normalized description of the direct effect of key aerosol types on solar radiation as estimated from AERONET aerosols and MODIS albedos, *J. Geophys. Res., 110,* D19202, doi:10.1029/2005JD005909.

Tables:

Table 1: Comparisons of the fine-mode fractions at 550 nm for individual aerosol types derived from Terra MODIS Collection 4 and 5.

Aerosol types	Collection 5	Collection 4
Pollution	0.90	0.92
Mineral dust	0.37	0.51
Marine aerosol	0.45	0.32

Table 2: Estimated uncertainties in the derived anthropogenic aerosol optical depth (τ_a) at 550 nm resulting from uncertainties associated with individual parameters in Eq. (1). The overall uncertainty is estimated by assuming that the probability distribution function for each factor is log normal and individual sources of uncertainty are independent (following Penner et al., 1994).

Parameters	Estimated uncertainty	Resultant τ_a uncertainty	Uncertainty Factor (UF) for τ_a
τ	20%	26%	1.26
f_d	20%	12%	1.12
f_a	20%	27%	1.27
f_m	20%	20%	1.20
τ_m	50%	15%	1.15
Total uncertainty factor for $\tau_a = e^{(\sum_i (\log UF_i)^2)^{1/2}} = 1.52$			

Table captions:

Table 1: Comparisons of the fine-mode fractions at 550 nm for individual aerosol types derived from Terra MODIS Collection 4 and 5.

Table 2: Estimated uncertainties in the derived anthropogenic aerosol optical depth (τ_a) at 550 nm resulting from uncertainties associated with individual parameters in Eq. (1). The overall uncertainty is estimated by assuming that the probability distribution function for each factor is log normal and individual sources of uncertainty are independent (following Penner et al., 1994).

Figure Captions:

Figure 1: Frequency distribution of the f_m difference between using AOD at 550 nm of 0.15 and 0.10 as the upper bound in deriving the marine aerosol fine-mode fraction.

Figure 2: Distributions of marine aerosol fine-mode fraction (f_m) at 550 nm for December-January-February (DJF, left column) and June-July-August (JJA, right column) as derived from 2001-2007 Terra/MODIS Collection 5 Level 3 daily 1°x1° data (a-b) and simulated by GOCART (c-d) and GMI (e-f) model. For these GOCART and GMI simulations, size-segregated sea salt and sulfates produced from ocean dimethylsulfide (DMS) and volcanic SO_2 are considered to represent the marine aerosol. Sulfate is assumed to be exclusively fine-mode.

Figure 3a: 7-year (2001-2007) climatology of seasonal average anthropogenic aerosol optical depth at 550 nm, derived from Terra/MODIS Collection 5 data by using the MODIS-based temporal and spatially varying marine fine-mode fraction (f_m) as shown in Figure 2.

Figure 3b: 7-year seasonal averages of anthropogenic AOD (1st row), fine-mode fraction (2nd row), and anthropogenic fraction (3rd row), all at 550 nm, over ocean in 13 zones (light blue background).

Figure 4: Comparison of the derived anthropogenic AOD at 550 nm using the spatially and seasonally varying marine fine-mode fraction (f_m) with that using the constant f_m. Each of 52 (=13x4) data points represents a seasonal average over one of 13 zones defined in Figure 3b.

Figure 5: 2001-2007 average seasonal cycle of MODIS-derived anthropogenic AOD at 550 nm over different latitude bands.

Figure 6: Variations of de-seasonalized anthropogenic AOD at 550 nm over the seven-year period in different regions. A linear regression is performed, shown as a solid line in the figure along with regression equation and correlation coefficient.

Figure 7: Comparison of 2002 annual average anthropogenic AOD at 550 nm over ocean derived in this study (a) and B08 (b), both from Terra MODIS Collection 5 data, and from GOCART simulations (c).

$f_m[0.15] - f_m[0.10]$
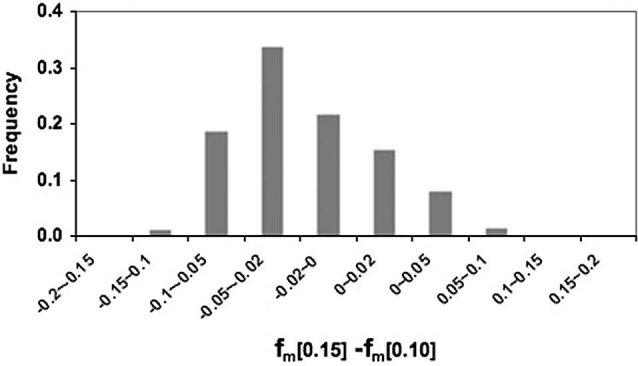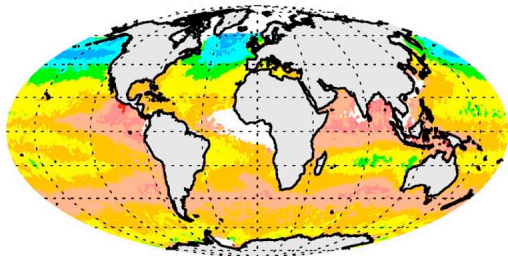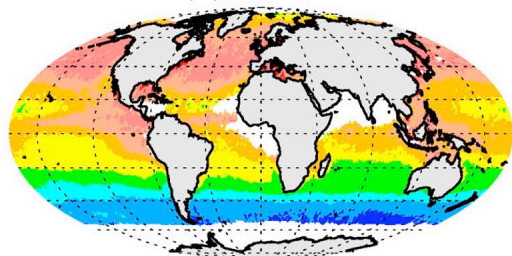
DJF	JJA
(a) MODIS	**(b) MODIS**
(c) GOCART	**(d) GOCART**
(e) GMI	**(f) GMI**

0.0 0.1 0.2 0.3 0.4 0.5 0.6 0.7 0.8 0.9 1.0

0.0 0.1 0.2 0.3 0.4 0.5 0.6 0.7 0.8 0.9 1.0

(a) DJF

0 .02 .04 .06 .08 .10 .15 .20 .30 .50 1.0

(b) MAM

0 .02 .04 .06 .08 .10 .15 .20 .30 .50 1.0

(c) JJA

0 .02 .04 .06 .08 .10 .15 .20 .30 .50 1.0

(d) SON

0 .02 .04 .06 .08 .10 .15 .20 .30 .50 1.0
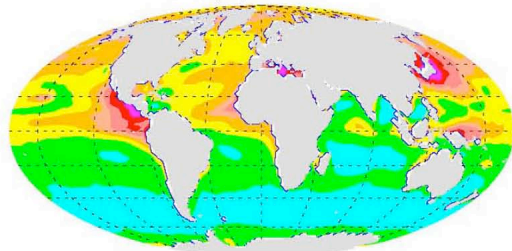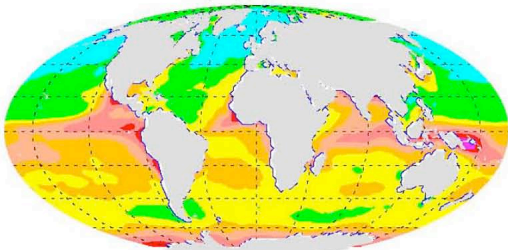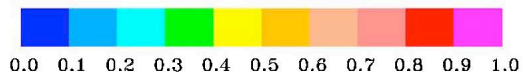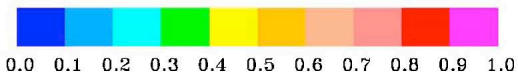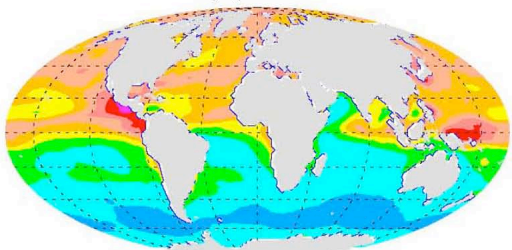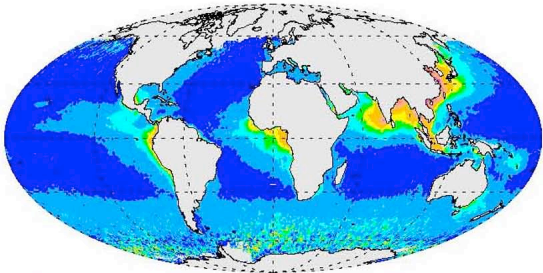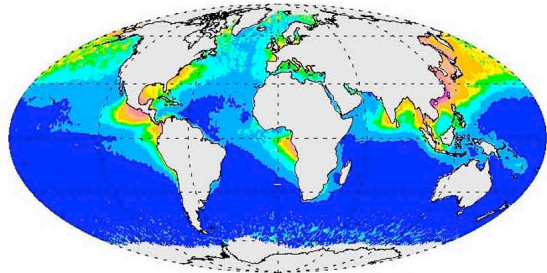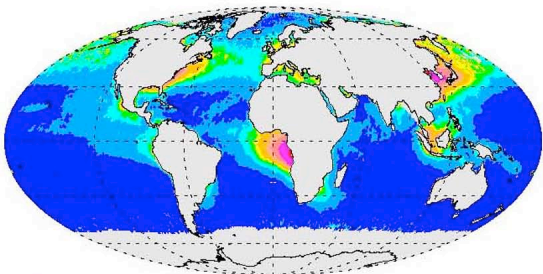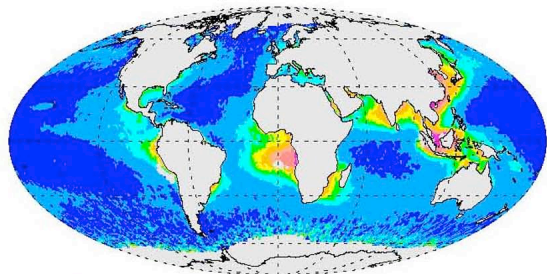
DJF	MAM	JJA	SON
0.011	0.062	0.068	0.027
0.265	0.508	0.635	0.424
0.056	0.229	0.382	0.183

DJF	MAM	JJA	SON
0.015	0.060	0.096	0.025
0.302	0.527	0.647	0.431
0.084	0.262	0.437	0.163

DJF	MAM	JJA	SON
0.041	0.099	0.134	0.067
0.478	0.622	0.697	0.568
0.250	0.359	0.497	0.345

DJF	MAM	JJA	SON
0.046	0.109	0.137	0.077
0.428	0.567	0.662	0.521
0.191	0.308	0.476	0.336

DJF	MAM	JJA	SON
0.027	0.049	0.036	0.033
0.461	0.500	0.522	0.524
0.203	0.240	0.249	0.259

DJF	MAM	JJA	SON
0.030	0.037	0.040	0.039
0.441	0.458	0.467	0.517
0.157	0.162	0.171	0.219

DJF	MAM	JJA	SON
0.086	0.053	0.038	0.081
0.601	0.512	0.405	0.597
0.386	0.216	0.107	0.362

DJF	MAM	JJA	SON
0.041	0.054	0.039	0.059
0.463	0.504	0.487	0.552
0.195	0.248	0.220	0.291

DJF	MAM	JJA	SON
0.015	0.015	0.012	0.026
0.434	0.459	0.415	0.472
0.143	0.147	0.104	0.198

DJF	MAM	JJA	SON
0.029	0.023	0.032	0.059
0.465	0.492	0.459	0.568
0.204	0.185	0.185	0.348

DJF	MAM	JJA	SON
0.026	0.024	0.047	0.058
0.482	0.487	0.446	0.541
0.202	0.190	0.212	0.306

DJF	MAM	JJA	SON
0.030	0.033	0.033	0.067
0.483	0.530	0.469	0.546
0.233	0.301	0.303	0.308

DJF	MAM	JJA	SON	
0.038	0.013	0.016	0.029	(Anthrop. AOD)
0.500	0.269	0.217	0.411	(Fine-mode fraction)
0.223	0.072	0.081	0.150	(Anthrop. fraction)

Figure showing anthrop AOD time series for four latitude bands (DJF, MAM, JJA, SON) from 2001 to 2007.

(a) 30N-60N
$y = 0.0003x - 0.0041$
$R^2 = 0.0524$

(b) Eq-30N
$y = 0.0005x - 0.0069$
$R^2 = 0.412$

(c) 30S-Eq
$y = 0.0003x - 0.004$
$R^2 = 0.3744$

(d) 60S-60N
$y = 0.0003x - 0.0037$
$R^2 = 0.2735$
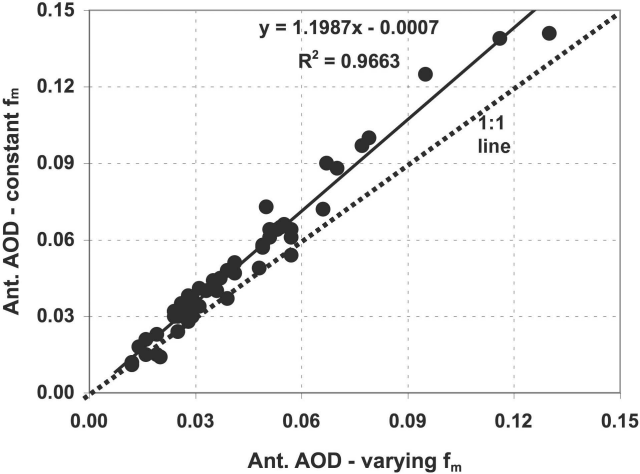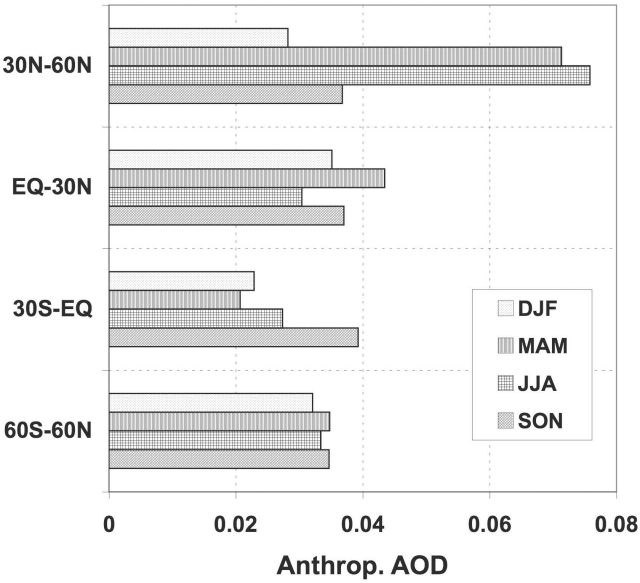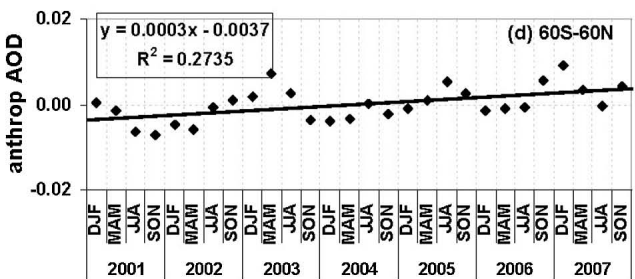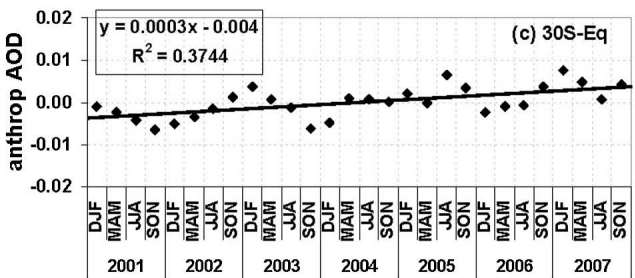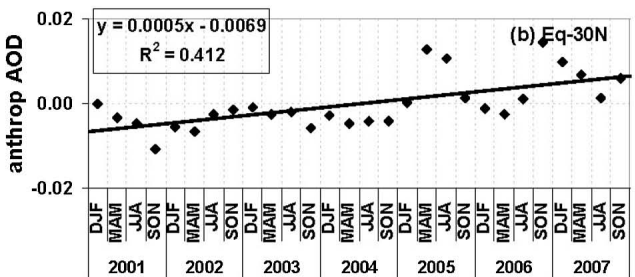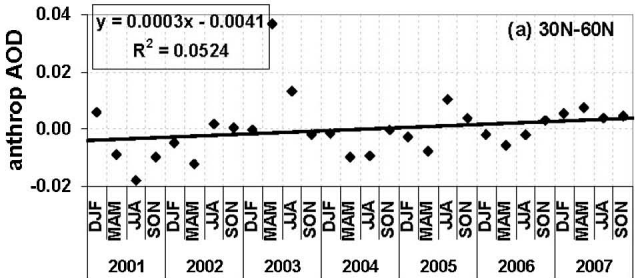
(a) This study
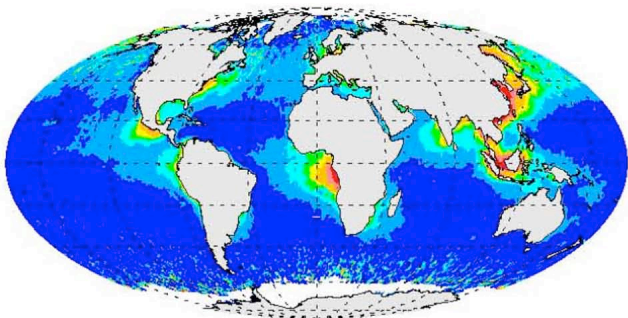
(b) B08
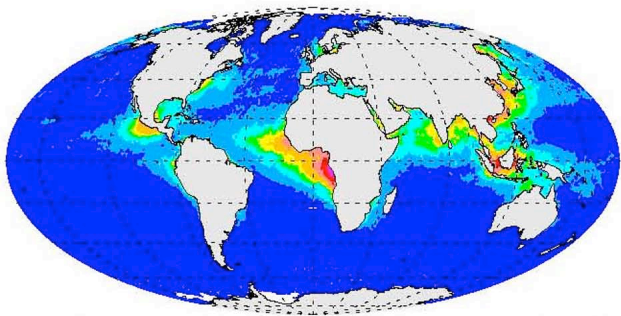
(c) GOCART
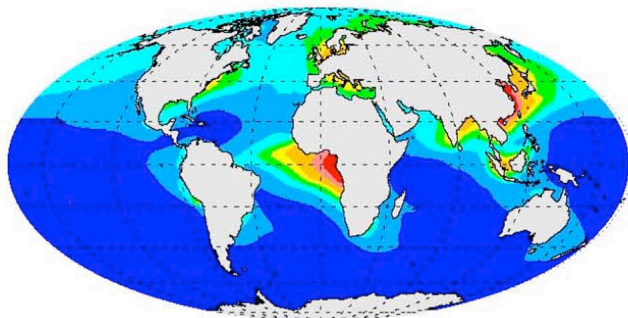
0.0 0.02 0.04 0.06 0.08 0.10 0.15 0.2 0.3 0.5